

Figure S1a. ORTEP View of **2** (ellipsoids at the 50% probability level). Hydrogen atoms have been omitted for clarity.

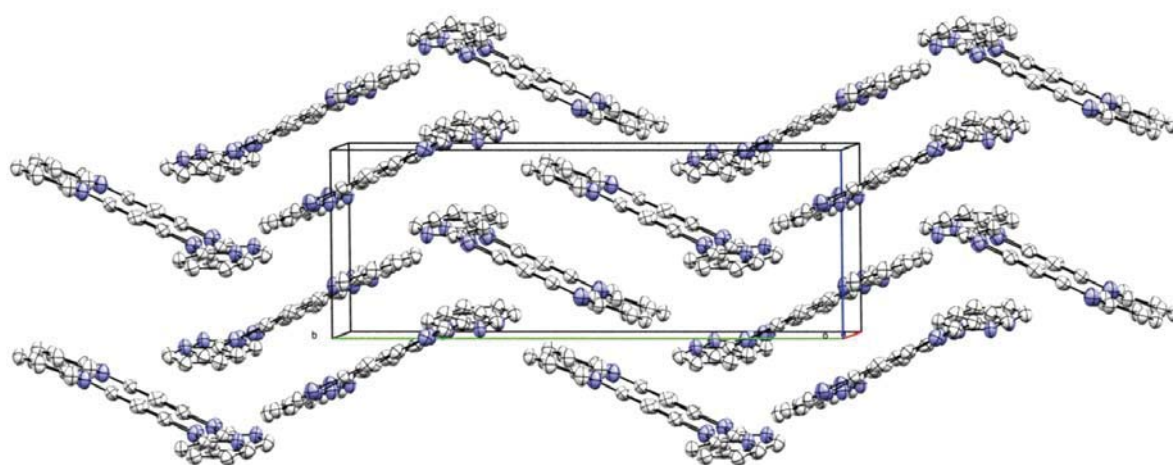


Figure S1b. Packing diagram of compound **2** seen along the a-axis (ellipsoids at the 50% probability level). Hydrogen atoms have been omitted for clarity.

Table S1. Selected interatomic distances (Å) and angles (°) for compound **2**.

C1–N1	1.3808(17)	C5–C4	1.388(2)
C1a–N1a	1.3787(17)	C5a–C4	1.386(2)
C1–N2	1.2968(19)	N1–C11	1.4150(17)
C1a–N2a	1.2983(19)	N1a–C11a	1.4172(17)
N1–C2	1.3976(17)		
N1a–C2a	1.4000(17)	N1–C1–N2	114.4(1)
N2–C5	1.3965(18)	N1a–C1a–N2a	114.7(1)
N2a–C5a	1.4107(19)	C1–N1–C11	124.3(1)
C2–C3	1.3879(18)	C1a–N1a–C11a	125.9(1)
C2a–C3	1.3852(19)		
C2–C5	1.4136(18)	C1...C1a	6.449(2)
C2a–C5a	1.4107(19)		

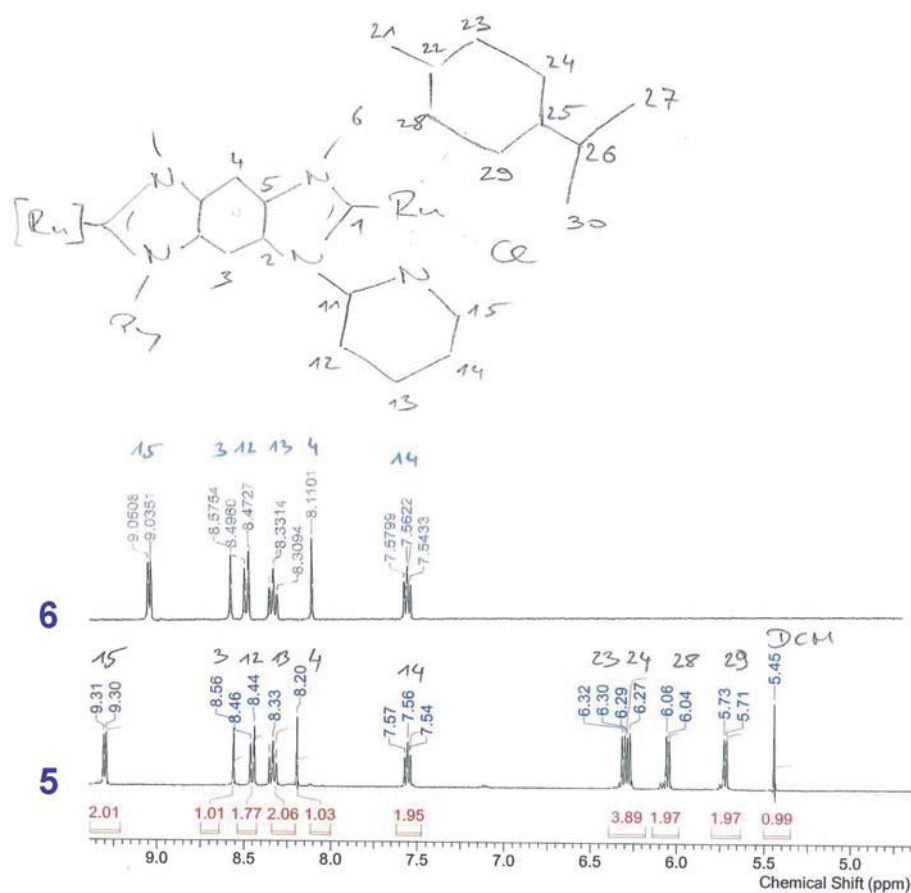


Figure S2. Stacked ^1H NMR plots of the aromatic section of complexes **5** (diastereopure, bottom) and **6** (top).

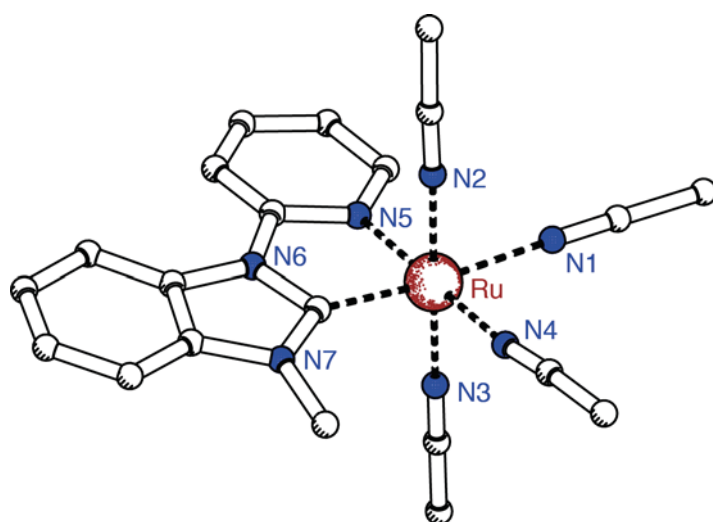


Figure S3. Pluton drawing of one of the four crystallographically independent complex cations of **9**. Severe disorder in the anions could not be refined to acceptable levels, which prevents a full discussion of data. The bite angle of **9** is in the expected range (78.5° in average over the four independent residues, cf Table 2). The bonds between the ruthenium center and the solvent ligands also follow the same trend as observed in **6**, with the MeCN trans to the carbene markedly more distant from the Ru center than the other three MeCN ligands: Ru–C1 1.97; Ru–N1 2.12; Ru–N2 2.04; Ru–N3 2.03; Ru–N4 2.01; Ru–N5 2.06;

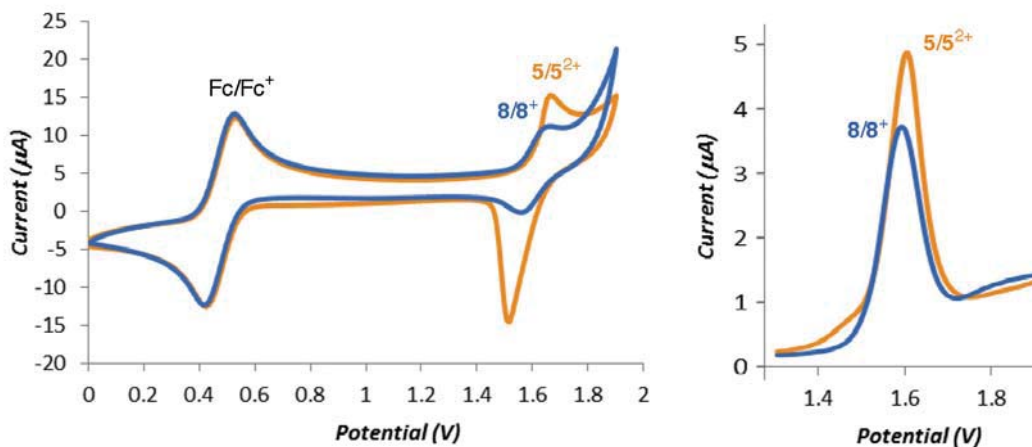


Figure S4. CV diagram (left) and DPV measurement (right) of complexes **5** and **8** (ca. 1 mM) in dry CH_2Cl_2 with 0.1 M $[\text{NBu}_4][\text{PF}_6]$ as supporting electrolyte at 100 mV s^{-1} scan rate; Fc^+/Fc used as internal reference.

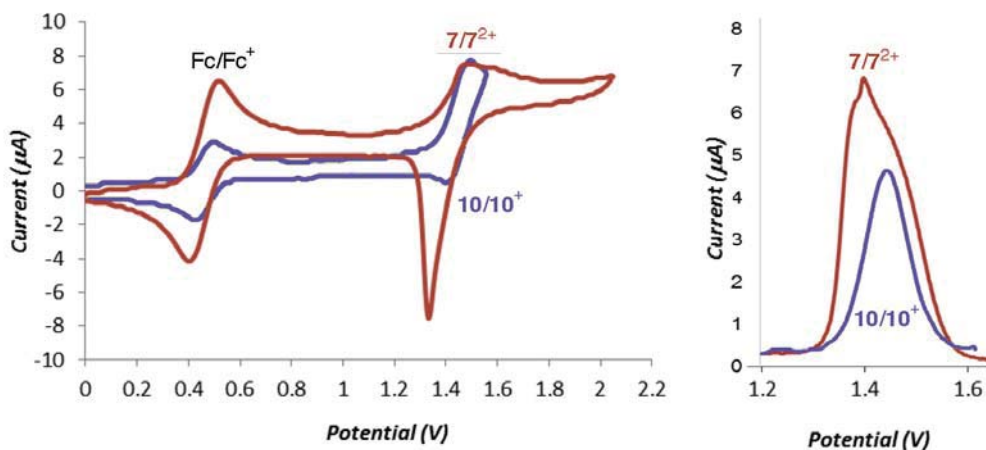


Figure S5. CV (left) and DPV (right) plot of complexes **7** and **10** (ca. 1 mM) in dry CH_2Cl_2 with 0.1 M $[\text{NBu}_4][\text{PF}_6]$ as supporting electrolyte, 50 mV s^{-1} scan rate (Fc^+/Fc used as internal standard, $E_{1/2}(\text{Fc}/\text{Fc}^+) = 0.41 \text{ V}$ vs. SCE).

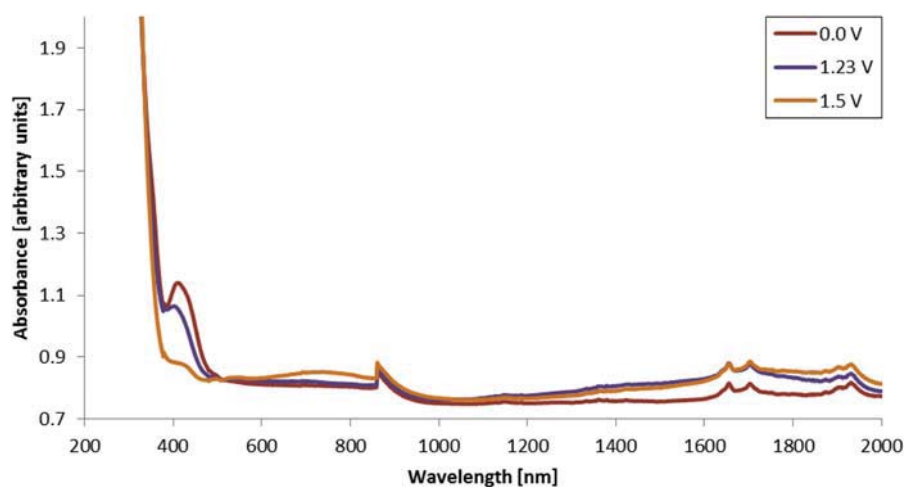


Figure S6. Absorption spectra of complexes **7** at 0.0 V, 7^+ at +1.23 V and 7^{2+} at +1.5 V (MeNO_2 solution).

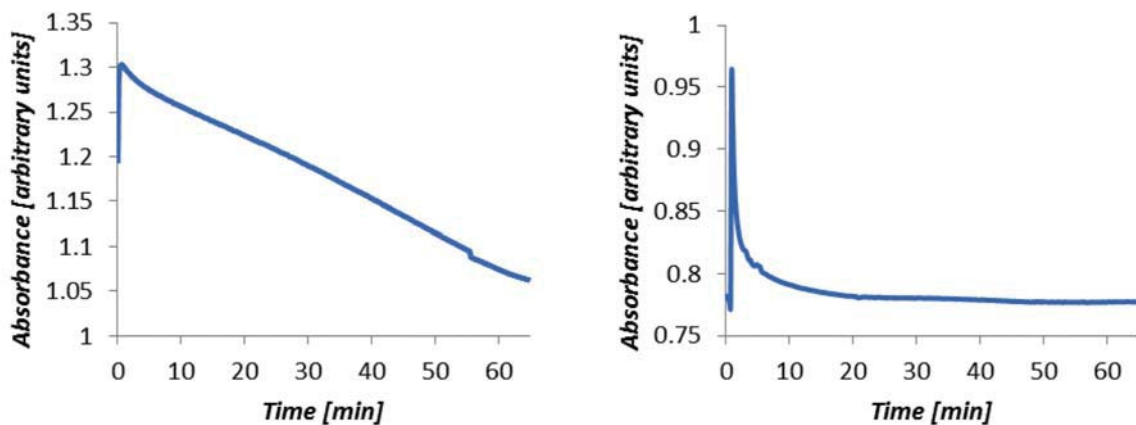


Figure S7. Stability tests: MV species 6^+ at 1.46 V observed at 1590 nm (left). Fully oxidized 6^{2+} species at 1.6 V observed at 820 nm (right).

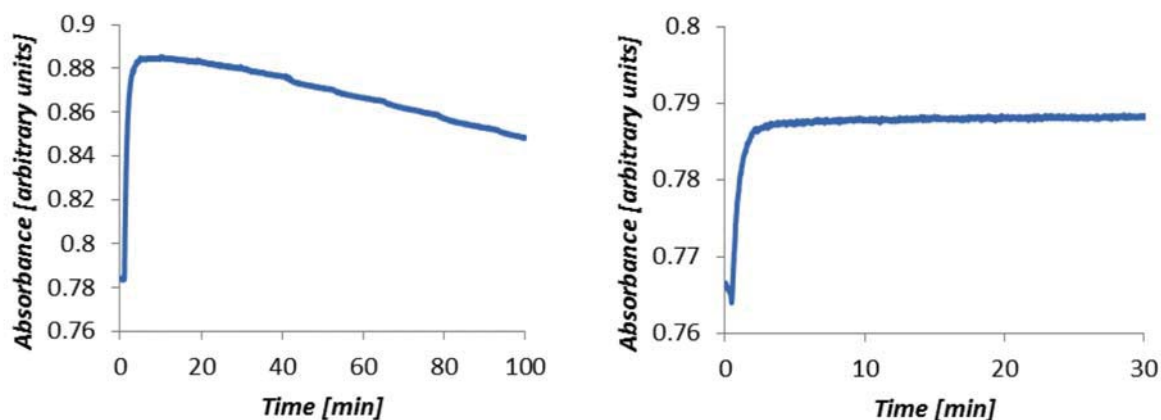


Figure S8. Stability tests: MV species 7^+ at 1.23 V observed at 1730 nm (left). Dication 7^{2+} at 1.5 V observed at 740 nm (right).

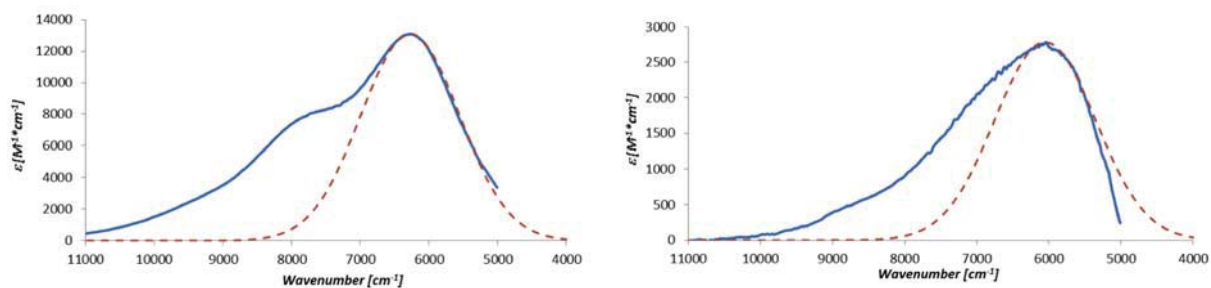


Figure S9. IVCT band of the mixed-valent species 6^+ (left) 7^+ (right; blue solid lines) and corresponding (symmetric) Gaussian fitting curves (red dashed lines; normalized to experimentally determined extinction coefficient at λ_{max} standard deviation 700 cm^{-1} and 720 cm^{-1} , respectively). The poor fit demonstrates the asymmetric shape of the IVCT band.

Table S2. Crystallographic data for compounds **2**, **6**, and **10**.

	2	6	10
CCDC No.			
mol formula	C ₁₈ H ₁₂ N ₆	C ₅₂ H ₆₄ F ₂₄ N ₂₂ P ₄ Ru ₂	C ₃₃ H ₂₇ F ₁₂ N ₇ P ₂ Ru
Crystal system	Monoclinic	Monoclinic	Triclinic
Space group	<i>P2₁/c</i>	<i>P2₁/c</i>	<i>P₋₁</i>
Unit cell			
a /Å	9.2616(4)	12.154(2)	10.4632(9)
b /Å	20.3317(6)	28.597(6)	12.4848(13)
c /Å	7.5352(3)	21.640(4)	18.8260(15)
α /°	90	90	97.959(8)
β /°	96.336(3)	90.03(3)	103.187(6)
γ /°	90	90	114.396(6)
Volume /Å ³	1410.24(9)	7521(3)	2104.2(3)
Z	4	4	2
T /K	200	100	150
μ /mm ⁻¹	0.09	0.60	0.79
Abs. corr.	none	numerical	Numerical
Total reflecons	19196	13538	15954
Unique reflecons	2652	13538	7309
parameters	217	956	551
R ₁ ^{a)} [I>2σ(I)]	0.0388,	0.0657	0.0585
wR ₂ ^{b)} [I>2σ(I)]	0.1024	0.1556	0.1401
GOOF	1.048	0.979	1.049
ρ _{fin} (max, min) /e Å ⁻³	0.18, -0.20	0.77, -0.87	0.81, -0.69

^{a)} $R_1 = \Sigma ||F_O| - |F_C|| / \Sigma |F_O|$.

^{b)} $wR_2 = [\Sigma w(F_O^2 - F_C^2)^2 / \Sigma (w(F_O^2)^2)]^{1/2}$; $w = 1 / [\sigma^2(F_O^2) + (ap)^2 + bp]$; $p = (F_O^2 + 2F_C^2) / 3$.